

# Cosmological tensions and $Q_{\text{CDM}}$ as an alternative to $\Lambda\text{CDM}$

---

**Amin Aboubrahim<sup>a</sup> and Pran Nath<sup>b,\*</sup>**

<sup>a</sup>*Department of Physics and Astronomy, Union College,  
807 Union Street, Schenectady, NY 12308, U.S.A.*

<sup>b</sup>*Department of Physics, Northeastern University,  
111 Forsyth Street, Boston, MA 02115-5000, U.S.A.*

*E-mail: [abouibra@union.edu](mailto:abouibra@union.edu), [p.nath@northeastern.edu](mailto:p.nath@northeastern.edu)*

The Standard Model of cosmology,  $\Lambda\text{CDM}$ , while enormously successful, is currently unable to account for several cosmological anomalies the most prominent of which are in the measurements of the Hubble parameter and  $S_8$ . Additionally, the inclusion of the cosmological constant is theoretically unappealing. This has led to extensions of the model such as the use of fluid equations for interacting dark matter and dark energy which, however, are ad hoc since they do not appear to arise from a Lagrangian. Recently, we have proposed  $Q_{\text{CDM}}$  as an alternative to  $\Lambda\text{CDM}$  which is a dynamical model of a quintessence field interacting with dark matter within a field theoretic approach. In this approach, we analyze the effect of the dark matter mass, the dark matter-dark energy interaction strength and the dark matter self-interaction on the cosmological parameters. Further, within  $Q_{\text{CDM}}$  we investigate the possible alleviation of the Hubble tension and the  $S_8$  anomaly and the nature of dark energy.

*Proceedings of the Corfu Summer Institute 2024 "School and Workshops on Elementary Particle Physics and Gravity" (CORFU2024) 12 - 26 May, and 25 August - 27 September, 2024  
Corfu, Greece*

---

\*Speaker

## 1. Introduction

The  $\Lambda\text{CDM}$  model has been successful in explaining a wide range of cosmological data but has recently faced challenges in explaining some anomalies, the most prominent of which are a discrepancy in measurements of the Hubble parameter (known as the Hubble tension) and  $S_8$ . To take account of the latter, many works directly use continuity equations for dark matter and dark energy with sources chosen to satisfy the overall energy conservation. However, such approaches do not have any fundamental origin. More specifically, the fluid equations currently in use have no simple field-theoretic basis. In this note, we discuss a field-theoretic formulation of interacting dark matter and dark energy proposed in ref. [1] which is fully field-theoretic as an alternative to  $\Lambda\text{CDM}$ . For specificity we will discuss an explicit model of two interacting spin zero fields, one for dark matter and the other for dark energy. In this framework we compute the background and linear perturbation equations within this field-theoretic formalism. We then carry out numerical fits to the cosmological data which include data from Planck [2] (with lensing), BAO, Pantheon, SHOES, and WiggleZ, and specifically discuss the  $H_0$  and  $S_8$  tensions. At the end we will summarize our results and draw some conclusions.

## 2. $\Lambda\text{CDM}$ and the fluid equations

The Lagrangian of  $\Lambda\text{CDM}$  is given by  $\mathcal{L} = \frac{1}{16\pi G}(R - 2\Lambda) + \mathcal{L}_{\text{CDM}}$  and contains no direct interaction between dark matter and dark energy. In models of quintessence, the  $\Lambda$  term is replaced by a dynamical spin zero field. In the so-called two-fluid model, one adopts the continuity equations for dark matter and dark energy with the inclusion of source terms which are chosen so that the total energy is conserved. Often the fluid equations do not specifically refer to fields but deal directly with energy densities and the equations of state. However, it is important to consider what the assumptions of the fluid equations are by looking at their explicit form within a field-theoretic formulation. Thus, we consider two spin zero fields, one of which is a quintessence dark energy field and the other a dark matter field and assume there is a coupling between them. In this case the continuity equations that follow from them are given by

$$\mathcal{D}_\alpha T_\phi^{\alpha\beta} = J_\phi^\beta, \quad (\text{DE}); \quad \mathcal{D}_\alpha T_\chi^{\alpha\beta} = J_\chi^\beta, \quad (\text{DM}). \quad (1)$$

In a Lagrangian theory with an interaction between the  $\phi$  and  $\chi$  fields, the source terms  $J_\phi^\beta$  and  $J_\chi^\beta$  are determined by the Lagrangian equations of motion and in general do not satisfy the simple relation  $J_\phi^\beta = -J_\chi^\beta$ . However, the conservation of energy-momentum is automatic in a Lagrangian formulation and does not need to be imposed by hand. We contrast this with the fluid equations currently in use where, one assumes no underlying Lagrangian, but adopts the expressions of Eq. (1) with the constraint  $J_\phi^\beta = -J_\chi^\beta$  which is introduced in an ad hoc manner. On the other hand all the fundamental theories of physics are based on Lagrangians and an action principle. This includes the Standard Model of particle physics, Einstein theory, and string theory. So the fluid model as currently used cannot be considered a fundamental cosmological model.

### 3. $Q_{\text{CDM}}$ as an alternative to $\Lambda\text{CDM}$

As mentioned earlier we discuss now a Lagrangian formulation of interacting dark matter (DM) and dark energy (DE) as an alternative to  $\Lambda\text{CDM}$ . We will use a specific model of DM and DE as an illustrative example but the underlying formalism is valid for any field-theoretic choice of DM and DE. Thus as an illustrative example of  $Q_{\text{CDM}}$  we consider a Lagrangian formulation of interacting two spin zero DM and DE fields whose action and total potential are given by

$$A = \int d^4x \sqrt{-g} \left[ -\frac{1}{2} \phi'^{\mu} \phi_{,\mu} - \frac{1}{2} \chi'^{\mu} \chi_{,\mu} - V(\phi, \chi) \right], \quad (2)$$

$$V(\phi, \chi) = V_1(\chi) + V_2(\phi) + V_3(\phi, \chi). \quad (3)$$

This is a fairly general form of the Lagrangian for two interacting spin zero fields. We will specify the forms of the potentials when we carry out the numerical analysis later. For the background we consider a flat, homogeneous and isotropic universe characterized by the Friedmann-Robertson-Walker (FRW) metric written in conformal time so that

$$ds^2 = g_{\mu\nu} dx^{\mu} dx^{\nu} = a^2 (-d\tau^2 + \gamma_{ij} dx^i dx^j), \quad (4)$$

where  $a$  is time-dependent scale factor;  $\gamma_{ij}$  are spatial components of the metric; and  $\tau$  is the conformal time, so that  $d\tau = dt/a(t)$ . The background fields satisfy the following KG equations

$$\chi_0'' + 2\mathcal{H}\chi_0' + a^2(\bar{V}_1 + \bar{V}_3)_{,\chi} = 0, \text{ and } \phi_0'' + 2\mathcal{H}\phi_0' + a^2(\bar{V}_2 + \bar{V}_3)_{,\phi} = 0, \quad (5)$$

where  $\bar{V}(\phi, \chi) \equiv V(\phi_0, \chi_0)$  and  $\bar{V}_{1,\chi} \equiv (V_{1,\chi})_{\chi=\chi_0}$ , etc; and  $\mathcal{H} = aH$ , with  $H = \dot{a}/a$ . The field theory model gives the following DE and DM continuity equations

$$\rho'_{\phi} + 3\mathcal{H}(1 + w_{\phi})\rho_{\phi} = Q_{\phi}, \quad (\text{DE}) \quad (6)$$

$$\rho'_{\chi} + 3\mathcal{H}(1 + w_{\chi})\rho_{\chi} = Q_{\chi}, \quad (\text{DM}) \quad (7)$$

where the source terms are  $Q_{\phi} = \bar{V}_{3,\chi}\chi'$  and  $Q_{\chi} = \bar{V}_{3,\phi}\phi'$ . Energy conservation requires that the total energy density is

$$\rho' + 3\mathcal{H}(1 + w)\rho = 0, \quad (8)$$

with  $\rho$  defined in such a way to avoid double counting, i.e.,  $\rho = \rho_{\phi} + \rho_{\chi} - V_3$ .

We note here that in the two-fluid model one sets  $Q_{\phi} = -Q_{\chi} = Q$  so that the fluid equations assume the form

$$\rho'_{\phi} + 3\mathcal{H}(1 + w_{\phi})\rho_{\phi} = Q, \quad (\text{DE}) \quad (9)$$

$$\rho'_{\chi} + 3\mathcal{H}(1 + w_{\chi})\rho_{\chi} = -Q. \quad (\text{DM}). \quad (10)$$

While the assumption  $Q_{\phi} = -Q_{\chi} = Q$  guarantees energy conservation, the constraint  $Q_{\phi} = -Q_{\chi}$  is ad hoc, and makes the model non-Lagrangian.

#### 4. Linear perturbations

We discuss now linear perturbations around the background of the spin zero fields so that

$$\chi(t, \vec{x}) = \chi_0(t) + \chi_1(t, \vec{x}) + \dots, \quad \phi(t, \vec{x}) = \phi_0(t) + \phi_1(t, \vec{x}) + \dots \quad (11)$$

Perturbations of the metric in a general gauge is given by

$$g^{00} = -a^{-2}(1 - 2A), \quad g^{0i} = -a^{-2}B^i, \quad g^{ij} = a^{-2}(\gamma^{ij} - 2H_L\gamma^{ij} - 2H_T^{ij}), \quad (12)$$

where  $A$  is a scalar potential,  $B^i$  a vector shift,  $H_L$  is a scalar perturbation to the spatial curvature and  $H_T^{ij}$  is a trace-free distortion to the spatial metric. There are two types of gauges that are generally assumed in the analysis. These are the synchronous and conformal (or Newtonian) gauges. In the synchronous gauge  $g^{00}$  and  $g^{0i}$  are not perturbed and so the line element has the form:  $ds^2 = a^2(\tau) [-d\tau^2 + (\delta_{ij} + h_{ij})dx^i dx^j]$ , while  $A = B = 0$ ,  $H_L = \frac{1}{6}h$ , where  $h$  is trace of the metric perturbations  $h_{ij}$ . The conformal (Newtonian) gauge is characterized by  $B = H_T = 0$ ,  $A \equiv \Psi$ ,  $H_L \equiv \Phi$ . Our analysis is carried out in a general gauge which can then reduce to either the synchronous gauge and or the conformal gauge based on the above prescription.

The perturbations of the stress-energy tensor is given by

$$T_\nu^\mu = \bar{T}_\nu^\mu + \delta T_\nu^\mu, \quad (13)$$

where the stress tensor in component form is given by

$$T_0^0 = -\rho - \delta\rho, \quad T_i^0 = (\rho + p)(v_i - B_i), \quad (14)$$

$$T_0^i = -(\rho + p)v_i, \quad T_j^i = (p + \delta p)\delta_j^i + p\Pi_j^i, \quad (15)$$

with  $\Pi_j^i$  representing the anisotropic stress,  $v_i$  the 3-velocity,  $\delta\rho$  and  $\delta p$  being the density and pressure perturbations. The off-diagonal element  $\delta T_i^0$  gives the velocity divergence so that

$$\delta T_i^0 = -a^{-2}\phi'_0\delta\phi_{,i}, \quad (16)$$

where the velocity divergence  $\theta$  is defined in Fourier space so that  $\theta = ik^i v_i$  or alternately  $\Theta \equiv (1 + w)\theta$  are determined by

$$\rho_\phi\Theta_\phi = \frac{k}{a^2}\phi'_0\phi_1, \quad \rho_\chi\Theta_\chi = \frac{k}{a^2}\chi'_0\chi_1. \quad (17)$$

The first order perturbations  $\phi_1$  and  $\chi_1$  are determined via the solutions to the KG equations they satisfy which are

$$\phi_1'' + 2\mathcal{H}\phi_1' + (k^2 + a^2\bar{V}_{,\phi\phi})\phi_1 + a^2\bar{V}_{,\phi\chi}\chi_1 + 2a^2\bar{V}_{,\phi}A + (3H_L' - A' + kB)\phi_0' = 0, \quad (18)$$

$$\chi_1'' + 2\mathcal{H}\chi_1' + (k^2 + a^2\bar{V}_{,\chi\chi})\chi_1 + a^2\bar{V}_{,\chi\phi}\phi_1 + 2a^2\bar{V}_{,\chi}A + (3H_L' - A' + kB)\chi_0' = 0. \quad (19)$$

Using the above, one computes the density perturbations defined so that

$$\delta_i \equiv \frac{\delta\rho_i}{\bar{\rho}_i} = \frac{\rho_i(t, \vec{x}) - \bar{\rho}_i(t)}{\bar{\rho}_i}, \quad (20)$$

From here on we will assume specific forms of the potentials which are

$$V_1(\chi) = \frac{1}{2}m_\chi^2\chi^2 + \frac{\lambda}{4}\chi^4, \quad (\text{DM}), \quad (21)$$

$$V_2(\phi) = \mu^4 \left[ 1 + \cos\left(\frac{\phi}{F}\right) \right], \quad (\text{DE}), \quad (22)$$

$$V_3(\phi, \chi) = \frac{\tilde{\lambda}}{2}\chi^2\phi^2, \quad (\text{DM-DE interaction}). \quad (23)$$

One straightforward approach is to solve the Klein-Gordon equations, and then compute the densities and other relevant cosmological quantities. However, this approach can be time consuming in certain regions of the parameter space. Thus a relevant parameter in the time evolution of the fields is the Hubble time  $\mathcal{H}^{-1}$  relative to  $m_\chi^{-1}$ . For the case when  $m_\chi^{-1} \ll \mathcal{H}^{-1}$ , one encounters rapid oscillations in the DM field, making the computations intractable. To overcome this, it is found preferable to directly solve the differential equations for the density perturbations  $\delta_i$  and the velocity variance  $\Theta_i$  averaged over a period of rapid oscillations. For the  $\chi$  field, the evolution of the density perturbations is given by

$$\begin{aligned} \delta'_\chi = & \left[ 3\mathcal{H}(w_\chi - c_{s\chi}^2) - \frac{Q_\chi}{\rho_\chi} \right] \delta_\chi + \frac{3\mathcal{H}Q_\chi}{\rho_\chi(1+w_\chi)}(c_{s\chi}^2 - c_{\chi\text{ad}}^2)\frac{\Theta_\chi}{k} - 9\mathcal{H}^2(c_{s\chi}^2 - c_{\chi\text{ad}}^2)\frac{\Theta_\chi}{k} - \Theta_\chi k \\ & + \frac{a^2}{k} \frac{\rho_\phi}{\rho_\chi} \bar{V}_{3,\phi\phi} \Theta_\phi + \frac{1}{\rho_\chi} \bar{V}_{3,\chi\phi} \phi'_0 \chi_1 + \frac{1}{\rho_\chi} \bar{V}_{3,\phi\phi} \phi'_1 - (3H'_L + kB)(1+w_\chi), \end{aligned} \quad (24)$$

while for the velocity divergence one gets

$$\begin{aligned} \Theta'_\chi = & (3c_{s\chi}^2 - 1)\mathcal{H}\Theta_\chi + k\delta_\chi c_{s\chi}^2 + 3\mathcal{H}(w_\chi - c_{\chi\text{ad}}^2)\Theta_\chi \\ & - \frac{Q_\chi}{\rho_\chi} \left( 1 + \frac{c_{s\chi}^2 - c_{\chi\text{ad}}^2}{1+w_\chi} \right) \Theta_\chi + \frac{k}{\rho_\chi} \bar{V}_{3,\phi\phi} \phi_1 + k(1+w_\chi)A. \end{aligned} \quad (25)$$

In the analysis above two types of sound speeds enter in the equations, i.e.,  $c_{s\chi}^2$  and  $c_{\chi\text{ad}}^2$  where  $c_{s\chi}^2$  is defined so that  $c_{s\chi}^2 = \delta p_\chi / \delta \rho_\chi$ , and  $c_{\chi\text{ad}}^2$  depends on the equation of state  $w_\chi$ . Thus  $c_{\chi\text{ad}}^2$  is given by

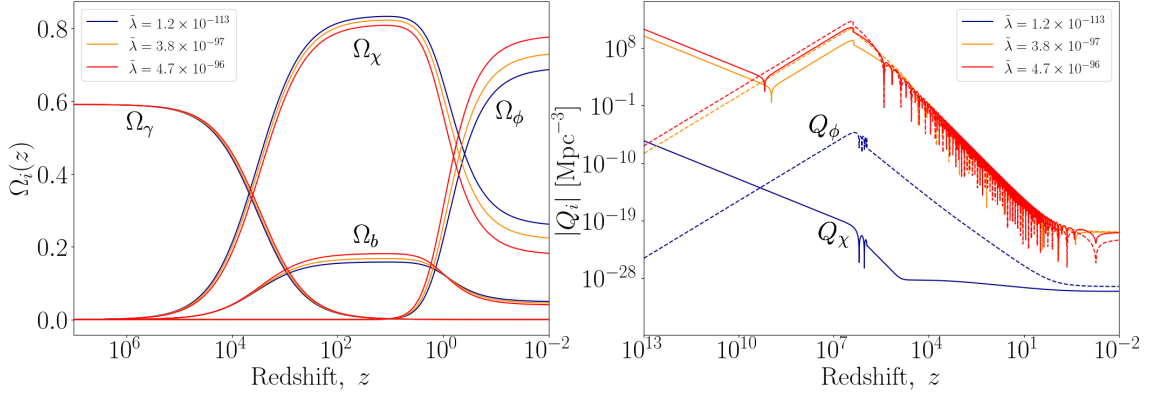
$$c_{\chi\text{ad}}^2 \equiv \frac{p'_\chi}{\rho'_\chi} = w_\chi - \frac{w'_\chi \rho_\chi}{3\mathcal{H}(1+w_\chi)\rho_\chi - Q_\chi}, \quad \text{with} \quad w_\chi^{-1} = 3 + \frac{8m_\chi^4}{9\lambda\langle\rho_\chi\rangle} \left( 1 + \frac{\tilde{\lambda}\phi_0^2}{m_\chi^2} \right). \quad (26)$$

We note that in the absence of self-interactions,  $\lambda = 0$ , which gives  $w_\chi = 0$  and CDM is pressureless as expected. However, in the limit when  $\frac{8m_\chi^4}{9\lambda}\langle\rho_\chi\rangle \ll 1$  one finds  $w_\chi \rightarrow \frac{1}{3}$  and in this case the  $\chi$  field behaves as radiation. This is checked numerically in the analysis.

## 5. Numerical analysis and fits to cosmological data

We discuss the numerical analysis of the cosmological parameters in two parts. First, we consider a few benchmarks to study in detail the effect of dark energy interaction with dark matter on the cosmological parameters. In the second part we will run a Markov Chain Monte Carlo

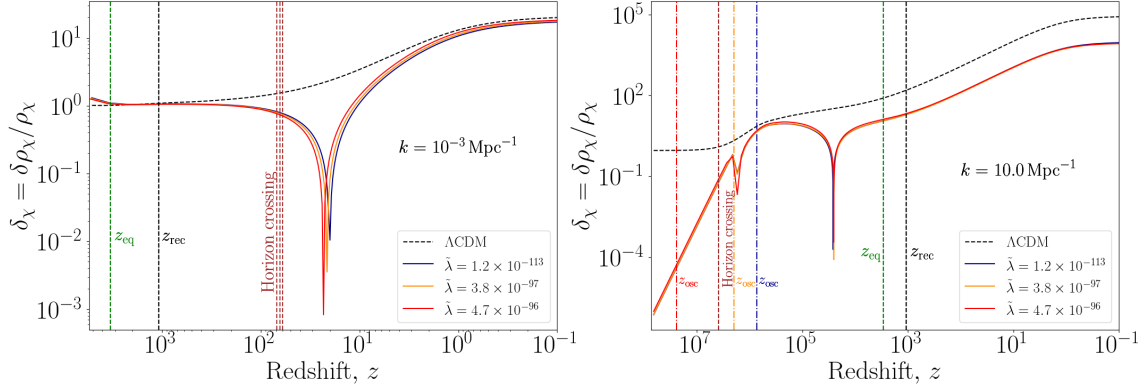
analysis and use Bayesian inference to extract the cosmological parameters. We use the input parameters:  $\mu, F, m_\chi, \lambda, \tilde{\lambda}; \phi_{\text{ini}}, \phi'_{\text{ini}}; \chi_{\text{ini}}, \chi'_{\text{ini}}; a_{\text{ini}} \sim 10^{-14}$ . Here the background fields for dark matter and dark energy are evolved from early times to late times including the contributions from neutrinos, baryons, and radiation. The analysis utilizes the Boltzmann solver CLASS [3] to evolve the background and perturbations equations. We have carried out a full numerical analysis where we investigate the effects of varying  $\lambda, \tilde{\lambda}, m_\chi$  on a number of cosmological quantities of interest which consist of  $Q_\phi, Q_\chi, \delta_\chi, \Theta_\chi, H(z), w_\phi, w_\chi, \Omega_\phi, \Omega_\chi, \Omega_\gamma, \Omega_b, P(k), \frac{\ell(\ell+1)}{2\pi} C_\ell^{TT}$ . However, in this note we exhibit only a subset of the results which we next discuss, and a complete analysis can be found in ref. [1].



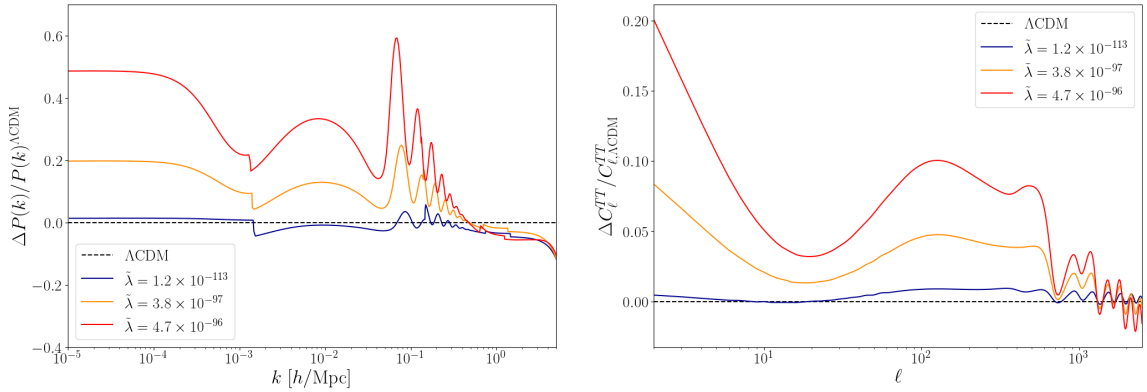
**Figure 1:** The left panel exhibits the energy density fraction of dark matter, dark energy, baryons and radiation as a function of the redshift for three DM-DE couplings  $\tilde{\lambda}$ . The right panel exhibits plots of sources  $Q_\phi$  and  $Q_\chi$  as a function of the redshift for the same three couplings of the dark matter-dark energy interaction strengths as the left panel.

Fig. 1 exhibits the sensitivity of the cosmological parameters on the dark matter-dark energy interaction strength  $\tilde{\lambda}$ . Here the left panel shows the evolution of the energy density fractions  $\Omega_\phi, \Omega_\chi, \Omega_\gamma, \Omega_b$  as a function of the redshift  $z$  from early times to current times. The figure shows that the energy density fractions  $\Omega_\phi$  and  $\Omega_\chi$  are sensitively dependent on  $\tilde{\lambda}$ . The right panel exhibits the evolution of the sources  $Q_\phi$  and  $Q_\chi$  over a wide range of redshifts and one finds that  $Q_\phi + Q_\chi \neq 0$  over this entire range which contradicts the assumption usually made, i.e., that  $Q_\phi = -Q_\chi = Q$  in the two-fluid models. Next we analyze the effect of DM-DE interaction on the density perturbations of dark matter  $\delta_\chi$  as a function of the redshift  $z$ . This is exhibited in Fig. 2 for two values of  $k$ :  $k = 10^{-3} \text{ Mpc}^{-1}$  (left panel) and  $k = 10.0 \text{ Mpc}^{-1}$  (right panel) for the same set of  $\tilde{\lambda}$  as in Fig. 1. In the left panel one can see that DM-DE interaction has little effect on the mode at superhorizon scale but the effect becomes more prominent after horizon entry where the perturbations corresponding to different interaction strengths become distinct before increasing and tracing  $\Lambda\text{CDM}$  again. In the right panel, the mode starts to oscillate as it enters the horizon causing a suppression of growth. Once the mode becomes sub-Jeans, the pressure in the fluid drops and the perturbations grow, trending in the direction of  $\Lambda\text{CDM}$  while remaining suppressed in comparison to CDM. The dark vertical line marked  $z_{\text{rec}}$  indicates the point in  $z$  where recombination occurs, the red vertical line marked  $z_{\text{eq}}$  indicated the point of matter-radiation equality, and the blue vertical line indicates the point where the  $k$  mode enters the horizon and begins to affect structure formation.

In the left panel of Fig. 3, we show the relative difference in the matter power spectrum between our model and  $\Lambda\text{CDM}$  for the three benchmarks. Here one finds that the effect of DM-DE interaction on the matter power spectrum is not significant except for  $k < k_{\text{eq}}$  which corresponds to large scales. The right panel of Fig. 3 gives the relative difference in the temperature power spectrum between our model and  $\Lambda\text{CDM}$  as a function of the multipoles also for three benchmarks of DM-DE interactions. Here also one finds that the effect of DM-DE interactions are typically small; specifically the acoustic peak is not much affected relative to the  $\Lambda\text{CDM}$  prediction. However, a significant effect is visible for small  $\ell$  values.



**Figure 2:** Plots showing the dark matter density perturbations for two values of  $k$ :  $k = 10^{-3} \text{ Mpc}^{-1}$  (left panel) and  $k = 10.0 \text{ Mpc}^{-1}$  (right panel), as a function of the redshift  $z$  and for three values of  $\tilde{\lambda}$ . The three dotted vertical lines correspond to the time of horizon crossing (brown), matter-radiation equality (green) and re-combination (black). The three dash-dot vertical lines correspond to  $z_{\text{osc}}$ , the scale factor when oscillations of the field start, with colors corresponding to each of the three couplings for the dark matter-dark energy interactions.



**Figure 3:** Left panel: the relative difference in the matter power spectrum between our model and  $\Lambda\text{CDM}$  plotted against the wavenumber  $k$  for three couplings of dark matter-dark energy interactions. Right panel: the relative difference in the temperature power spectrum between our model and  $\Lambda\text{CDM}$  as a function of the multipoles also for three benchmarks of dark matter-dark energy interactions. The dashed line represents the  $\Lambda\text{CDM}$  model.

## 6. MCMC analysis for interacting dark matter-dark energy using $Q_{\text{CDM}}$ model

Before giving our analysis of the cosmological parameters, we discuss briefly some of the tensions appearing in cosmological data. Thus, currently there is a discrepancy in some observables arising from a mismatch between their inferred values from analysis of the CMB based on  $\Lambda\text{CDM}$  [4–6] and their local direct measurements [7, 8]. Specifically, a  $5\sigma$  discrepancy is seen for the Hubble parameter between the Planck collaboration [9] result and the SH0ES collaboration [10] using Cepheid-calibrated supernovae. Another discrepancy relates to the clustering of matter at large scales observed from galaxy clustering and weak gravitational lensing surveys [11–16] which are seen to be discrepant with the analyses using matter clustering power from the CMB anisotropies based on  $\Lambda\text{CDM}$ . A relevant parameter is  $S_8$  defined as  $S_8 \equiv \sigma_8 \sqrt{\Omega_m}/0.3$  which is the weighted amplitude of the variance in matter fluctuations for spheres of size  $8h^{-1}\text{Mpc}$ . Currently  $S_8$  shows a  $2-3\sigma$  tension between the local measurements and the those from CMB using  $\Lambda\text{CDM}$ . Additionally, the most recent results from DESI [17] points to a tension between the DE equation of state (EoS) as predicted by  $\Lambda\text{CDM}$  and that inferred from experiment where the EoS appears to be dynamical. We address the possibility of a dynamical EoS in ref. [18].

Before going further, we note that prior to the work of ref. [1] many models of DM-DE interaction have been presented. These include refs. [19–29]. Some of the works have used variational approach to introduce the couplings [30–33] while other works have used interactions at the level of continuity equations for the energy densities treating both DM and DE as fluids [34–41], DM is a fluid while DE is quintessence [42–45] and both DM and DE are scalar fields [46–49]. A recent review of several models can be found in [50].

$Q_{\text{CDM}}$  is different from previous works in that it is fully field-theoretic with no extraneous ad hoc assumptions made in fluid equations. We give now the result of our analysis within  $Q_{\text{CDM}}$ . The data sets used in our analysis are as follows: the Planck data on anisotropies and polarization measurements [4, 9, 51] and Planck lensing data [52]. For Baryon Acoustic Oscillation (BAO) the data sets from the Sloan Digital Sky Survey is used which includes several surveys [53–58]. For Pantheon+SH0ES the data sets are from [10, 59]. For WiggleZ, the Large Scale Structure data survey is used [60]. Using the data sets above we perform a MCMC fit to the cosmological data in five different combinations and we look for the best fits to the cosmological parameters of our model while examining the effect they have on other important parameters such as:  $H_0, \Omega_m, \Omega_\phi, \sigma_8, S_8$ . To check the goodness of the fits we define:

$$\Delta\chi_{\min}^2 = \chi_{\min, Q_{\text{CDM}}}^2 - \chi_{\min, \Lambda\text{CDM}}^2. \quad (27)$$

The result of the analysis is exhibited in Tables 1–3.



Data sets/Theory	$\Delta\chi_{\text{min}}^2$
Planck + BAO	0.0
Planck+ Lensing	0.0
Planck + Pantheon + SH0ES	-1.0
Planck+ Lensing + BAO+ WiggleZ	+1.0
All data sets	-1.0

**Table 1:** Comparison of  $Q_{\text{CDM}}$  analysis with that of  $\Lambda\text{CDM}$ .

Data sets/Theory	$H_0$
SH0ES	$H_0^{\text{R22}} = (73.04 \pm 1.04)\text{km/s/Mpc}$
Planck	$H_0^{\text{Pl}} = (67.4 \pm 0.5)\text{km/s/Mpc}$
$Q_{\text{CDM}}$	$H_0 = (68.84^{+2.10}_{-0.24})\text{ km/s/Mpc}$

**Table 2:** Comparison of  $Q_{\text{CDM}}$  analysis for  $H_0$  with those of Planck and SH0ES.

In Table 1, we give a comparison of the goodness of  $Q_{\text{CDM}}$  fits relative to that of  $\Lambda\text{CDM}$ . Here the first two data sets show no difference between  $Q_{\text{CDM}}$  and  $\Lambda\text{CDM}$ . The third data set and the combination of all data show that  $Q_{\text{CDM}}$  fits the data better, although only slightly as exhibited in Table 1. In Table 2, we give a comparison between the values of  $H_0$  in our  $Q_{\text{CDM}}$  model and those obtained by Planck and SH0ES. Here the  $H_0$  tension in  $\Lambda\text{CDM}$  with R22 is more than  $5\sigma$ , while the  $H_0$  from our analysis based on  $Q_{\text{CDM}}$  is now  $\sim 2.7\sigma$  away from the R22 measurement indicating a slight improvement in reducing the tension. In Table 3, we discuss the  $S_8$  tension. Here one finds that the  $Q_{\text{CDM}}$  analysis (using the Planck + Pantheon + SH0ES data sets) is consistent with both KiDS and DES, and resolves the  $\sim 3\sigma$  tension that  $S_8$  has with the Standard Model. A similar result in resolving the  $S_8$  tension is based on including a drag term between DM and DE is discussed in ref. [61].

Data sets/Theory	$S_8$
Planck	$S_8^{\text{Pl}} = 0.834 \pm 0.016$
KiDS-1000	$S_8^{\text{KiDS}} = 0.759^{+0.024}_{-0.021}$
DES-Y3	$S_8^{\text{DES}} = 0.759^{+0.025}_{-0.023}$
$Q_{\text{CDM}}$	$S_8 = 0.7975^{+0.0180}_{-0.0250}$

**Table 3:** Comparison of  $Q_{\text{CDM}}$  analysis for  $S_8$  with those of Planck, KiDS-1000 and DES-Y3.

## 7. Conclusion

The two-fluid model for dark matter and dark energy which uses an ad hoc assumption of an interaction between them at the level of the continuity equations, does not arise from an underlying

Lagrangian and is not at the same footing as the Standard Model of particle physics or Einstein's gravity. We have discussed an alternative approach, i.e.,  $Q_{\text{CDM}}$ , which is field-theoretic and produces a consistent set of continuity equations for dark matter and dark energy replacing the fluid equations currently in use. Thus the  $Q_{\text{CDM}}$  model provides the proper framework for cosmological analyses. We have carried out fits to the cosmological data using  $Q_{\text{CDM}}$  and find that the  $\chi^2$  of our fits to be at the same level as the  $\Lambda\text{CDM}$ . Observables such as the Hubble parameter and  $S_8$  are found to be sensitive to dark matter self-interaction as well as to DM-DE interactions and this helps alleviate the tension for  $H_0$  while resolving the  $S_8$  tension for some data sets.  $Q_{\text{CDM}}$  is theoretically robust and with more data we should be able to discriminate further  $Q_{\text{CDM}}$  from  $\Lambda\text{CDM}$ . Finally, in addition to the work discussed above, a new analysis discusses a new phenomenon related to the transmutation of dark energy from thawing to scaling freezing in the late universe [18].

## Acknowledgments

The research of PN was supported in part by the NSF Grant PHY-2209903.

## References

- [1] A. Aboubrahim and P. Nath, *Interacting ultralight dark matter and dark energy and fits to cosmological data in a field theory approach*, *JCAP* **09** (2024) 076, [[arXiv:2406.19284](#)].
- [2] **Planck** Collaboration, N. Aghanim et al., *Planck 2018 results. VI. Cosmological parameters*, *Astron. Astrophys.* **641** (2020) A6, [[arXiv:1807.06209](#)]. [Erratum: *Astron. Astrophys.* 652, C4 (2021)].
- [3] D. Blas, J. Lesgourgues, and T. Tram, *The Cosmic Linear Anisotropy Solving System (CLASS) II: Approximation schemes*, *JCAP* **07** (2011) 034, [[arXiv:1104.2933](#)].
- [4] **Planck** Collaboration, N. Aghanim et al., *Planck 2018 results. I. Overview and the cosmological legacy of Planck*, *Astron. Astrophys.* **641** (2020) A1, [[arXiv:1807.06205](#)].
- [5] **ACT** Collaboration, S. Aiola et al., *The Atacama Cosmology Telescope: DR4 Maps and Cosmological Parameters*, *JCAP* **12** (2020) 047, [[arXiv:2007.07288](#)].
- [6] **SPT-3G** Collaboration, L. Balkenhol et al., *Constraints on  $\Lambda\text{CDM}$  extensions from the SPT-3G 2018 EE and TE power spectra*, *Phys. Rev. D* **104** (2021), no. 8 083509, [[arXiv:2103.13618](#)].
- [7] A. G. Riess, S. Casertano, W. Yuan, L. M. Macri, and D. Scolnic, *Large Magellanic Cloud Cepheid Standards Provide a 1% Foundation for the Determination of the Hubble Constant and Stronger Evidence for Physics beyond  $\Lambda\text{CDM}$* , *Astrophys. J.* **876** (2019), no. 1 85, [[arXiv:1903.07603](#)].
- [8] **HOLiCOW** Collaboration, K. C. Wong et al., *HOLiCOW – XIII. A 2.4 per cent measurement of  $H_0$  from lensed quasars: 5.3 $\sigma$  tension between early- and late-Universe probes*, *Mon. Not. Roy. Astron. Soc.* **498** (2020), no. 1 1420–1439, [[arXiv:1907.04869](#)].

- [9] **Planck** Collaboration, N. Aghanim et al., *Planck 2018 results. VI. Cosmological parameters*, *Astron. Astrophys.* **641** (2020) A6, [[arXiv:1807.06209](#)]. [Erratum: *Astron. Astrophys.* 652, C4 (2021)].
- [10] A. G. Riess et al., *A Comprehensive Measurement of the Local Value of the Hubble Constant with  $1 \text{ km s}^{-1} \text{ Mpc}^{-1}$  Uncertainty from the Hubble Space Telescope and the SH0ES Team*, *Astrophys. J. Lett.* **934** (2022), no. 1 L7, [[arXiv:2112.04510](#)].
- [11] **KiDS** Collaboration, M. Asgari et al., *KiDS-1000 Cosmology: Cosmic shear constraints and comparison between two point statistics*, *Astron. Astrophys.* **645** (2021) A104, [[arXiv:2007.15633](#)].
- [12] S. Joudaki et al., *KiDS+VIKING-450 and DES-Y1 combined: Cosmology with cosmic shear*, *Astron. Astrophys.* **638** (2020) L1, [[arXiv:1906.09262](#)].
- [13] **DES** Collaboration, T. M. C. Abbott et al., *Dark Energy Survey Year 3 results: Cosmological constraints from galaxy clustering and weak lensing*, *Phys. Rev. D* **105** (2022), no. 2 023520, [[arXiv:2105.13549](#)].
- [14] C. Heymans et al., *KiDS-1000 Cosmology: Multi-probe weak gravitational lensing and spectroscopic galaxy clustering constraints*, *Astron. Astrophys.* **646** (2021) A140, [[arXiv:2007.15632](#)].
- [15] **DES** Collaboration, T. M. C. Abbott et al., *Dark Energy Survey Year 1 Results: Cosmological constraints from cluster abundances and weak lensing*, *Phys. Rev. D* **102** (2020), no. 2 023509, [[arXiv:2002.11124](#)].
- [16] L. Kazantzidis and L. Perivolaropoulos, *Evolution of the  $f\sigma_8$  tension with the Planck15/ $\Lambda\text{CDM}$  determination and implications for modified gravity theories*, *Phys. Rev. D* **97** (2018), no. 10 103503, [[arXiv:1803.01337](#)].
- [17] **DESI** Collaboration, A. G. Adame et al., *DESI 2024 VI: cosmological constraints from the measurements of baryon acoustic oscillations*, *JCAP* **02** (2025) 021, [[arXiv:2404.03002](#)].
- [18] A. Aboubrahim and P. Nath, *Transmutation of interacting quintessence in the late universe*, [arXiv:2411.11177](#).
- [19] A. Pourtsidou, C. Skordis, and E. J. Copeland, *Models of dark matter coupled to dark energy*, *Phys. Rev. D* **88** (2013), no. 8 083505, [[arXiv:1307.0458](#)].
- [20] A. Pourtsidou and T. Tram, *Reconciling CMB and structure growth measurements with dark energy interactions*, *Phys. Rev. D* **94** (2016), no. 4 043518, [[arXiv:1604.04222](#)].
- [21] M. S. Linton, A. Pourtsidou, R. Crittenden, and R. Maartens, *Variable sound speed in interacting dark energy models*, *JCAP* **04** (2018) 043, [[arXiv:1711.05196](#)].
- [22] F. N. Chamings, A. Avgoustidis, E. J. Copeland, A. M. Green, and A. Pourtsidou, *Understanding the suppression of structure formation from dark matter-dark energy momentum coupling*, *Phys. Rev. D* **101** (2020), no. 4 043531, [[arXiv:1912.09858](#)].

- [23] S. Pan, W. Yang, E. Di Valentino, E. N. Saridakis, and S. Chakraborty, *Interacting scenarios with dynamical dark energy: Observational constraints and alleviation of the  $H_0$  tension*, *Phys. Rev. D* **100** (2019), no. 10 103520, [[arXiv:1907.07540](#)].
- [24] M. Bonici and N. Maggiore, *Constraints on interacting dynamical dark energy and a new test for  $\Lambda$  CDM*, *Eur. Phys. J. C* **79** (2019), no. 8 672, [[arXiv:1812.11176](#)].
- [25] W. Yang, O. Mena, S. Pan, and E. Di Valentino, *Dark sectors with dynamical coupling*, *Phys. Rev. D* **100** (2019), no. 8 083509, [[arXiv:1906.11697](#)].
- [26] S. Pan, G. S. Sharov, and W. Yang, *Field theoretic interpretations of interacting dark energy scenarios and recent observations*, *Phys. Rev. D* **101** (2020), no. 10 103533, [[arXiv:2001.03120](#)].
- [27] B. Wang, E. Abdalla, F. Atrio-Barandela, and D. Pavon, *Dark Matter and Dark Energy Interactions: Theoretical Challenges, Cosmological Implications and Observational Signatures*, *Rept. Prog. Phys.* **79** (2016), no. 9 096901, [[arXiv:1603.08299](#)].
- [28] B. Wang, E. Abdalla, F. Atrio-Barandela, and D. Pavón, *Further understanding the interaction between dark energy and dark matter: current status and future directions*, *Rept. Prog. Phys.* **87** (2024), no. 3 036901, [[arXiv:2402.00819](#)].
- [29] K. Bamba, S. Capozziello, S. Nojiri, and S. D. Odintsov, *Dark energy cosmology: the equivalent description via different theoretical models and cosmography tests*, *Astrophys. Space Sci.* **342** (2012) 155–228, [[arXiv:1205.3421](#)].
- [30] C. G. Boehmer, N. Tamanini, and M. Wright, *Interacting quintessence from a variational approach Part I: algebraic couplings*, *Phys. Rev. D* **91** (2015), no. 12 123002, [[arXiv:1501.06540](#)].
- [31] C. G. Boehmer, N. Tamanini, and M. Wright, *Interacting quintessence from a variational approach Part II: derivative couplings*, *Phys. Rev. D* **91** (2015), no. 12 123003, [[arXiv:1502.04030](#)].
- [32] M. Archidiacono, E. Castorina, D. Redigolo, and E. Salvioni, *Unveiling dark fifth forces with linear cosmology*, *JCAP* **10** (2022) 074, [[arXiv:2204.08484](#)].
- [33] K. Rezazadeh, A. Ashoorioon, and D. Grin, *Cascading Dark Energy*, *Astrophys. J.* **975** (2024), no. 1 137, [[arXiv:2208.07631](#)].
- [34] W. J. Potter and S. Chongchitnan, *A Gauge-invariant approach to interactions in the dark sector*, *JCAP* **09** (2011) 005, [[arXiv:1108.4414](#)].
- [35] E. Di Valentino, A. Melchiorri, O. Mena, and S. Vagnozzi, *Nonminimal dark sector physics and cosmological tensions*, *Phys. Rev. D* **101** (2020), no. 6 063502, [[arXiv:1910.09853](#)].
- [36] E. Di Valentino, A. Melchiorri, O. Mena, and S. Vagnozzi, *Interacting dark energy in the early 2020s: A promising solution to the  $H_0$  and cosmic shear tensions*, *Phys. Dark Univ.* **30** (2020) 100666, [[arXiv:1908.04281](#)].

- [37] L. A. Escamilla, O. Akarsu, E. Di Valentino, and J. A. Vazquez, *Model-independent reconstruction of the interacting dark energy kernel: Binned and Gaussian process*, *JCAP* **11** (2023) 051, [[arXiv:2305.16290](#)].
- [38] A. Bernui, E. Di Valentino, W. Giarè, S. Kumar, and R. C. Nunes, *Exploring the  $H_0$  tension and the evidence for dark sector interactions from 2D BAO measurements*, *Phys. Rev. D* **107** (2023), no. 10 103531, [[arXiv:2301.06097](#)].
- [39] M. K. Sharma and S. Sur, *Dynamical system analysis of interacting dark energy-matter scenarios at the linearized inhomogeneous level*, *Phys. Dark Univ.* **40** (2023) 101192, [[arXiv:2112.14017](#)].
- [40] M. K. Sharma and S. Sur, *Imprints of interacting dark energy on cosmological perturbations*, *Int. J. Mod. Phys. D* **31** (2022), no. 03 2250017, [[arXiv:2112.08477](#)].
- [41] W. Yang, S. Pan, O. Mena, and E. Di Valentino, *On the dynamics of a dark sector coupling*, *JHEAp* **40** (2023) 19–40, [[arXiv:2209.14816](#)].
- [42] L. Amendola, *Coupled quintessence*, *Phys. Rev. D* **62** (2000) 043511, [[astro-ph/9908023](#)].
- [43] R. Kase and S. Tsujikawa, *Scalar-Field Dark Energy Nonminimally and Kinetically Coupled to Dark Matter*, *Phys. Rev. D* **101** (2020), no. 6 063511, [[arXiv:1910.02699](#)].
- [44] P. Pérez, U. Nucamendi, and R. De Arcia, *Revisiting dynamics of interacting quintessence*, *Eur. Phys. J. C* **81** (2021), no. 12 1063, [[arXiv:2104.07690](#)].
- [45] B.-H. Lee, W. Lee, E. O. Colgáin, M. M. Sheikh-Jabbari, and S. Thakur, *Is local  $H_0$  at odds with dark energy EFT?*, *JCAP* **04** (2022), no. 04 004, [[arXiv:2202.03906](#)].
- [46] G. Garcia-Arroyo, L. A. Ureña López, and J. A. Vázquez, *Interacting scalar fields: Dark matter and early dark energy*, *Phys. Rev. D* **110** (2024), no. 2 023529, [[arXiv:2402.08815](#)].
- [47] J. Beyer, S. Nurmi, and C. Wetterich, *Coupled dark energy and dark matter from dilatation anomaly*, *Phys. Rev. D* **84** (2011) 023010, [[arXiv:1012.1175](#)].
- [48] J. Beyer, *Linear Perturbations in a coupled cosmon-bolon cosmology*, [arXiv:1407.0497](#).
- [49] C. van de Bruck, G. Poulot, and E. M. Teixeira, *Scalar field dark matter and dark energy: a hybrid model for the dark sector*, *JCAP* **07** (2023) 019, [[arXiv:2211.13653](#)].
- [50] E. Abdalla et al., *Cosmology intertwined: A review of the particle physics, astrophysics, and cosmology associated with the cosmological tensions and anomalies*, *JHEAp* **34** (2022) 49–211, [[arXiv:2203.06142](#)].
- [51] **Planck** Collaboration, N. Aghanim et al., *Planck 2018 results. V. CMB power spectra and likelihoods*, *Astron. Astrophys.* **641** (2020) A5, [[arXiv:1907.12875](#)].
- [52] **Planck** Collaboration, N. Aghanim et al., *Planck 2018 results. VIII. Gravitational lensing*, *Astron. Astrophys.* **641** (2020) A8, [[arXiv:1807.06210](#)].

- [53] F. Beutler, C. Blake, M. Colless, D. H. Jones, L. Staveley-Smith, L. Campbell, Q. Parker, W. Saunders, and F. Watson, *The 6dF Galaxy Survey: Baryon Acoustic Oscillations and the Local Hubble Constant*, *Mon. Not. Roy. Astron. Soc.* **416** (2011) 3017–3032, [[arXiv:1106.3366](#)].
- [54] **BOSS** Collaboration, C. P. Ahn et al., *The Ninth Data Release of the Sloan Digital Sky Survey: First Spectroscopic Data from the SDSS-III Baryon Oscillation Spectroscopic Survey*, *Astrophys. J. Suppl.* **203** (2012) 21, [[arXiv:1207.7137](#)].
- [55] C. Howlett, A. Ross, L. Samushia, W. Percival, and M. Manera, *The clustering of the SDSS main galaxy sample – II. Mock galaxy catalogues and a measurement of the growth of structure from redshift space distortions at  $z = 0.15$* , *Mon. Not. Roy. Astron. Soc.* **449** (2015), no. 1 848–866, [[arXiv:1409.3238](#)].
- [56] A. J. Ross, L. Samushia, C. Howlett, W. J. Percival, A. Burden, and M. Manera, *The clustering of the SDSS DR7 main Galaxy sample – I. A 4 per cent distance measure at  $z = 0.15$* , *Mon. Not. Roy. Astron. Soc.* **449** (2015), no. 1 835–847, [[arXiv:1409.3242](#)].
- [57] **BOSS** Collaboration, S. Alam et al., *The clustering of galaxies in the completed SDSS-III Baryon Oscillation Spectroscopic Survey: cosmological analysis of the DR12 galaxy sample*, *Mon. Not. Roy. Astron. Soc.* **470** (2017), no. 3 2617–2652, [[arXiv:1607.03155](#)].
- [58] **eBOSS** Collaboration, S. Alam et al., *Completed SDSS-IV extended Baryon Oscillation Spectroscopic Survey: Cosmological implications from two decades of spectroscopic surveys at the Apache Point Observatory*, *Phys. Rev. D* **103** (2021), no. 8 083533, [[arXiv:2007.08991](#)].
- [59] D. Brout et al., *The Pantheon+ Analysis: Cosmological Constraints*, *Astrophys. J.* **938** (2022), no. 2 110, [[arXiv:2202.04077](#)].
- [60] D. Parkinson et al., *The WiggleZ Dark Energy Survey: Final data release and cosmological results*, *Phys. Rev. D* **86** (2012) 103518, [[arXiv:1210.2130](#)].
- [61] V. Poulin, J. L. Bernal, E. D. Kovetz, and M. Kamionkowski, *Sigma-8 tension is a drag*, *Phys. Rev. D* **107** (2023), no. 12 123538, [[arXiv:2209.06217](#)].